Malaysian Journal of Chemistry, 2016, Vol. 18(1), 46–59

Effects of Layers and Ratio Cs-TiO_2/Glass Photocatalyst towards Removal of Methylene Orange via Adsorption-photodegradation Process

Muhammad Nur Iman Amir, Nurhidayatullaili Muhd Julkapli*, Zul Adlan Mohd Hir and Sharifah Bee Abd Hamid

Nanotechnology and Catalysis Research Centre,
Institute of Post-graduate Studies, University of Malaya,
50603 Kuala Lumpur, Malaysia.

*Corresponding author (e-mail: nurhidayatullaili@um.edu.my)

Preparation of Cs-TiO_2 films by using glass substrate with synthesized TiO_2 and the study of photocatalytic activity of Cs-TiO_2 in the removal of methyl orange (MO) under the optimum conditions was conducted. Initially, TiO_2 nanoparticles was synthesized via sol gel methods and its chemical, physical and photocatalytic properties were characterized accordingly. This was divided into two parts which involved the as-synthesized sample (before calcination) — undergoing thermo-gravimetric analysis and then the same synthesized sample underwent Fourier transform infrared spectroscopy, X-ray diffraction and Raman spectroscopy analyses after it was calcined. Then, TiO_2 was incorporated with Cs solution in acidic medium before immobilized on glass substrate. UV-vis analysis was done to study the adsorption–photodegradation analysis of MO. It demonstrated that, the combination effects on adsorption–photodegradation process for the removal of MO occur promisingly when eight layers at 3:2 weight ratio (TiO_2:Cs) of Cs-TiO_2/glass photocatalyst was used for MO photodegradation. Approximately, 70% to 85% of total MO degradation by photocatalyst analysis was achieved. Therefore, a suitable photocatalytic conditions and sample parameters, possessing the Cs-TiO_2 gave the benefits of adsorption–photodegradation practice in the abatement of wastewater contaminants.

Key words: Adsorption-photodegradation; methylene orange; titanium dioxide nanoparticles; glass substrate

Received: October 2014; Accepted: February 2016

Water pollution from the domestic and industrial sectors continue to be a critical environmental and domestic problem [1]. In addition, confronted by increasingly more rigid rules, water pollution has become a major supply of issue as well as a concern with regard to industrial areas. Progress in industrialization in particular textile industries have led to the discharge of unprecedented amount of waste water containing synthetic dyes, which pollutes the rivers and consequently causes harm to human and other living organisms [2]. The azo reactive dye, that includes azo (–N=N–) groups associated with substituted aromatic structure which is sp^2 hybridized C-atoms was recognized as methyl orange (MO). Mostly, the azo groups tend to be bound to benzene or perhaps naphthalene rings. Sometimes, the azo groups also bind with aromatic heterocycles or enolizable aliphatic groups. MO is commonly used as an anionic monoazo dye in laboratory assays, textiles and other commercial products and has to be removed from water due to its toxicity [2, 6]. In view connected with it is high balance, MO is frequently employed as staining agent and titration indicator. For this reason, it had been chosen as a model pollutant in these research. MO and its breakdown products are toxic to living organisms [2]. Furthermore, dyes in wastewater are difficult to remove because they are stable to

light, heat and oxidizing agents. In short, they are not easily degradable [2]. The presence of ionizing groups known as auxochromes results in a much stronger alteration of the maximum absorption of the compound and provides a bonding affinity. Coloured dye waste water arises as a direct result of the production of the dye and because of its use in the textile and other industries. There are more than 100 000 commercially available dyes with over 7 × 105 of dyes produced annually worldwide [2]. Legislation that has been enacted on the discharge of MO (common dyes/pollutants), makes it then necessary to develop several efficient technologies for the removal of these pollutant from water or become wastewater [1]. There are several approaches of technologies and process to be used such as biological treatments, membrane process, advanced oxidation process, chemical and electrochemical technique [3]. Amongst them, photocatalysis procedure is the most common used for the removing of the metal and organic compound from industrial effluents, since the proper design of the catalyst and photoactivity process will enhance and produce high quality treated effluents [4]. Therefore, it is now labeled as an effective, efficient and economic method for the water separation analytical purpose and at the same time it can be used as decontamination applications.

Titanium oxide (TiO_2) nanoparticles or also known as Titania is a very well known and well researched material due to the stability of its chemical structure, biocompatibility, physical, optical, and electrical properties. Its photocatalytic properties have been utilized in various environmental applications to remove synthetic dyes from both water and air [5]. Nanocrystalline semiconductor TiO_2 particles are of interest due to their unique properties and several potential technological applications such as photocatalysis, sensors, solar cells and memory devices. There are several applicable uses of TiO_2 such as it exhibits good photo catalytic properties, hence is used in antiseptic and antibacterial compositions, degrading organic contaminants and germs, and as a UV-resistant material used in the paper industry for improving the opacity of paper.

It has been verified that so many aromatic compounds derived from synthetic dyes could be degraded successfully and effectively to be able to finalize more secure end products which are CO_2, H_2O, and also nutrient acids. While, adsorption process mediated simply by chitosan (Cs) is amongst the successful techniques that were effectively used by numerous pollutants which are inorganic, organic, and also heavy metal removal coming from wastewater. The combined effects between TiO_2 and Cs known as adsorption–photodegradation that is coated on a glass substrate (Cs-TiO_2/glass) as a improvement method for the treatment or pre-treatment of dye-containing wastewater that is under the illumination of visible light [6].

Besides that, it was reported that dyes, metal ions, organic acids, and pesticides are effectively adsorped by Cs because of its high adsorption potentials. A variety of useful features of Cs make it a versatile adsorbent. These features include its abundance, hydrophilicity, anti-bacterial property, biodegradability, non-toxicity and biocompability. Cs [β -(1-4)-2-amino-2-deoxy-d-glucose] being a hydrolyzed derivative of chitin contains high amount of amino ($–NH_2$) and hydroxyl (OH) functional groups. In fact, both $–NH_2$ and –OH groups on Cs chains could assist as coordination and reaction sites. The electrostatic attraction formed between the $–NH_2$ functional groups and the solutes can generate adsorption of organic substrates by Cs. Whereas, the chelating groups (the $–NH_2$ and –OH groups) on the Cs is attributed to the binding ability of that Cs for synthetic dyes .

In this study, the reactive TiO_2 that was synthesized by sol-gel method was coated and bound or incorporated with Cs onto the smooth surface of the glass substrate. It was expected that, this would be incredibly useful in the investigation of the mixed effect of adsorption–photodegradation mediated by Cs–TiO_2. The actual photocatalytic degradation process making use of TiO_2 was shown to be extremely successful to the degradation of MO as a model of synthetic dye compounds. Beside that, the presence of Cs was acknowledged to have a very encouraging

effect on the adsorption capability of the TiO_2 photocatalysis. Therefore, it was expected that both the individual advantages of TiO_2 and Cs own advantages could be matched together, hence, offering a diverse approach inside the abatement of several wastewater pollutants especially for synthetic dyes.

MATERIALS

Titanium isopropoxide (purity, 97%), $Ti[OCH(CH_3)_2]_4$ was used as a starting material to prepare/synthesis TiO_2 by sol-gel method and it was obtained from Sigma-Aldrich. Acetic acid (purity, 99%), CH_3CO_2H and sodium chloride, NaCl were obtained from Sigma-Aldrich.and Merck respectively. De-ionized water was used for preparing all standard solutions. Cs (medium molecular weight) were obtained from Sigma-Aldrich that was used for solution preparation of TiO_2- Cs/glass.

METHODOLGY

Synthesis of Nano-TiO_2 by Sol Gel Method

Titanium isopropoxide, Acetic acid glacial and deionized water were used for the preparation of nano-TiO_2 by sol gel method. Initially, TTIP (97%) solution, 2.8 ml was mixed in concentrated/ pure acid acetic acid glacial (>90%), 6 ml. After that TTIP was added slowly in acetic acid glacial solution. Next, DI water (36 ml) was added slowly under vigorous stirring, at ambient temperature, stirring rate of 350 rpm to 500 rpm for 4 h [9, 10].

Once, a clear solution was obtained (sol) the mixture was stirred for 1 h at 80°C [9]. To keep the reaction temperature constant, the beaker was covered with aluminium foil and thermometer was inserted into the surface of the mixture. Consequently, a solution was changed to gel at reaction temperature of 60°C.

As the reaction continued, the white suspension was obtained. The suspension was dried for overnight (12 h) at 80°C until amorphous and dried TiO_2 particles (yellowish colour) were obtained. Next, TiO_2 particles were manually ground with agate mortar. TiO_2 powder (0.70 g) were calcined for 5 h at 500°C and stored in controlled humidity and temperature conditions [7, 9].

Characterization of TiO_2 Nanoparticles Photocatalysis

To analyze the thermal behaviour of as-synthesized TiO_2, thermo-gravimetric analysis (TGA), Mettler toledo - TGA/SDTA851^e were conducted in Ar atmosphere at a heating rate of $10^oC\ min^{-1}$ from room temperature to 800°C. Besides that, Fourier transform infrared spectroscopy (FTIR) studies were carried out in the 400–4000 cm^{-1} wavenumber range in order to determine the chemical bondings in the catalyst structure of synthesized TiO_2. For the infrared absorption spectra, the samples were formed into pellets with KBr and the spectra were recorded on a Bruker FTIR spectrometer. The fine powder of synthesized TiO_2 was subjected to X-ray diffraction (XRD) and Raman spectroscopy analysis with Bruker-axs, Cu Kα radiation and Renishaw-inVia, NIR vibrations in the 800–50 cm^{-1} range, respectively to determine the crystal phase composition and crystallite size of the anatase materials of the TiO_2 used. Furthermore, the absorbance data of the MO samples were obtained from the optical spectra recorded on UV-VIS, Shimadzu - UV-3101PC with wavelengths ranging from 200–800 nm.

Preparation of Cs–TiO_2/Glass Substrate – Photocatalysts

Cs flake (0.25 g) was dissolved in a premixed solution of CH_3COOH (30 ml; 0.1 M) and NaCl (4 ml; 0.2 M) . The viscous solution was stirred continuously for 12 h to obtain a completely dissolved Cs flake. Then, TiO_2 powder (0.25 g) was added into the transparent viscous Cs solution. Subsequently, another CH_3COOH (5 ml; 0.1 M) was added [6]. The slurry was stirred continuously for 24 h to obtain the white cloudy viscous solution. The same procedure was repeated with different amounts (weight ratio between TiO_2 and Cs) of TiO_2 powder, the amount of TiO_2 powder being used were 0.125 g (1), 0.25 g (2) 0.375 g (3) and 0.5 g (4), but the amount of Cs were kept constant at 0.25 g (2). The ratio of TiO_2:Cs were 1:2, 2:2, 3:2 and 4:2, it was labelled as 2E1, 2E2, 2E3 and 2E4, respectively.

Glass substrate (25×75×2) mm were used as component to retain and fixed the prepared Cs–TiO_2 photocatalysts. The glass substrate was initially wiped clean thoroughly and dried up just before deposit. Then, the glass substrate were dipped in the TiO_2/Cs viscous solution with a uniform immersion rate manually and coated diameter (25×55) mm. The readily dipped glass substrate were dried at 100°C for 4 h alternately after each dipping process. Dipping process was repeated for 2, 4, 6 and 8 layers of TiO_2/Cs. Herein, the TiO_2 with Cs samples are called Cs-TiO_2/glass photocatalyst. Cs-TiO_2 thin film formed on the glass substrate was responsible for the adsorption and photodegradation reaction. Otherwise, the photocatalyst were stored in the dark to avoid pre-activation by room light or sunlight.

Photocatalytic Activity

The photocatalytic reaction was conducted in a 150 ml quartz cylindrical glass, at room temperature and humidity. Irradiation was provided by an UV lamp with wavelength of 365 nm, which are located at the center of the quartz glass. To achieve effective dispersion and ensure a constant dissolved O_2 concentration, the magnetic stirrer was placed at the bottom of the cylindrical glass and air was bubbled into the working solution from the bottom of the glass respectively (Figure 1). To evaluate the photocatalytic efficiency of Cs-TiO_2/Glass. The amount of TiO_2 and Cs together on the glass observed was about ≈0.01 g. The initial concentration of MO were 10 mg/l and 100 ml was used for the photodegradation process. The adsorption process was performed in the presence of catalyst under dark condition for about 15 min prior to photodegradation activity. About 5 ml of the sample solution was withdrawn at selected time intervals and the absorbance was measured directly by using UV-vis spectrophotometer (UV-3101PC Shimadzu) after done the adsorption-photodegradation process.

From the photocatalytic experiments, the percentage MO degraded by the prepared photocatalyst was determined from the following *Equation 1*:

$$\%\ \text{of methyl orange degradation} = (C_o - C_t)/C_o \times 100 \qquad (1)$$

Where, C_o is the initial concentration of MO and C_t is the concentration of MO after already finished the interval time ("t").

RESULT AND DISCUSSION

Characterization of TiO_2 Nanoparticles

As-synthesized sample of TiO_2 nanoparticles Using TGA. Figure 2 shows the TGA curve displaying the thermal analysis for as-synthesized TiO_2 . This analysis was employed to study the mass loss and chemical or physical changes

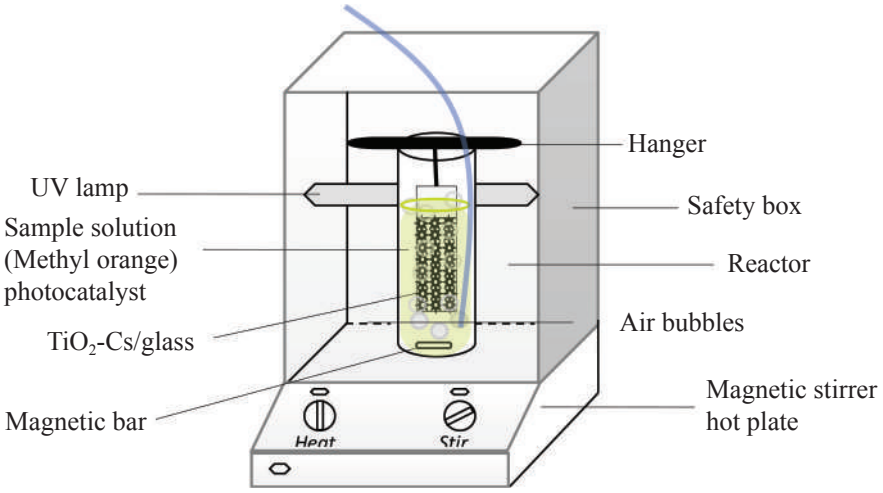

Figure 1. The photocatalytic reactor designed for MO adsorption-photodegradation.

of the nanomaterial as a function of increasing temperature or time. Based on the TGA curve, a significant weight loss was observed as the temperature increased from room temperature to 800°C which is attributed to the elimination of crystallized water and dehydration of water from TiO_2. With further increase of temperature, the mass loss rate slowed down and ceases at about 250°C. The first peak at 50°C indicates an endothermic event corresponding to the rapid release of moistrue - H_2O. The second peak at nearly 400°C presents the transformation of the precursors into the stable TiO_2 particles [17].

Synthesized sample of TiO_2 nanoparticles under FTIR, XRD and Raman spectroscopy. The FTIR spectra of synthesized TiO_2 is shown in Figure 3 through the FTIR spectra, peaks at 400 to 700 cm^{-1} were represented of O–Ti–O and Ti–O vibrations. It was shown that, the intensity of 700 to 400 cm^{-1} peaks were evidently increased due to the stretching vibration of Ti–O–Ti in anatase phase. The peaks centered at 1640 cm−1 and 3200 to 3700 cm^{-1} were characterized as the surface-adsorbed water (H_2O) and hydroxyl groups (-OH), respectively. There were some minor peak at 2900 cm^{-1} for curve of TiO_2 regarding C–H stretching band, which means there are some organic compounds remained in the sample of TiO_2 even after calcinations.

Figure 3 represents the FTIR spectra of synthesis TiO_2 after calcination process at 500°C for 5 h. The broad peaks at 3430 and 2360 cm^{-1} observed in dried gel sample have signatures of hydroxyl and carboxylic group, respectively. A broad peak at 700 cm^{-1} arises due to =C-H bending. After decomposition of gel at 500°C for 5 h, the product depicts a major peak at 470 cm^{-1} refer to the Figure 4, corresponding to Ti-O bond [7, 8].

The XRD patterns of synthesized TiO_2 for this study are presented in Figure 4. The spectra shows that the introduction of carbon material insignificantly affect the structure of the catalyst, due to the present of anatse phase in TiO_2. However, as the intensity of peaks decreased, the change in the crytsallinity of TiO_2 was observed, The change was contributed to the distribution of carbon compounds on the TiO_2 surface. The average crystallite size of prepared catalysts was calculated and tabulated in Table 1 by using the

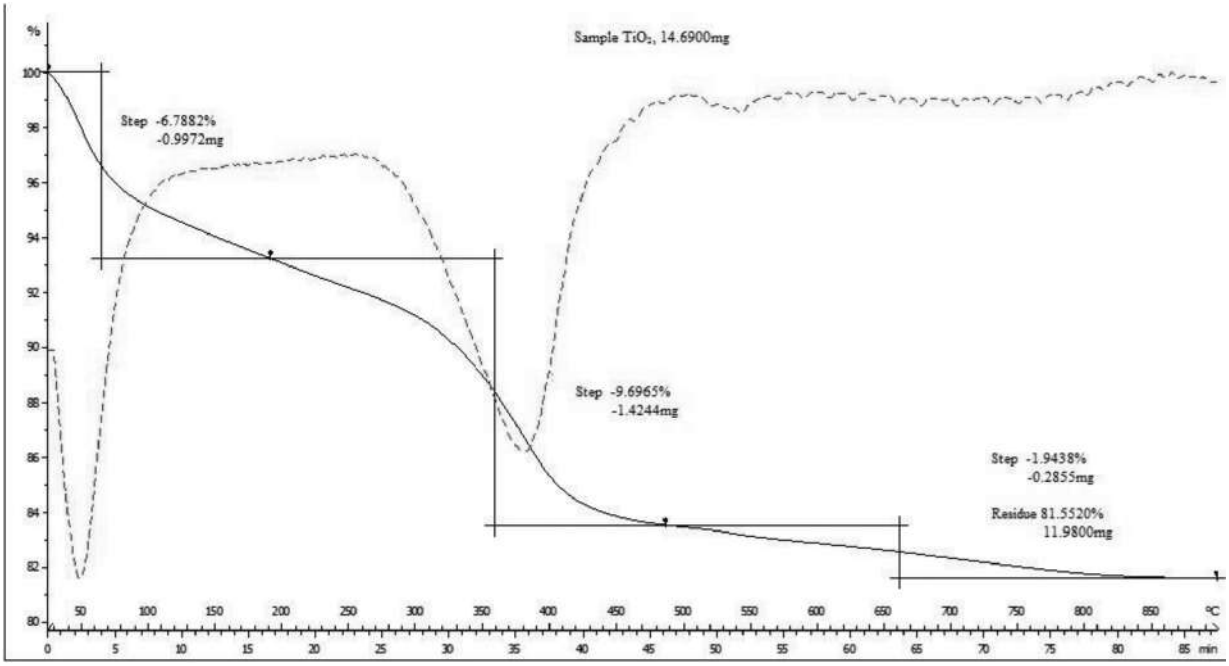

Figure 2. The result on TGA (for as-synthesized TiO_2 prepared with sol-gel method).

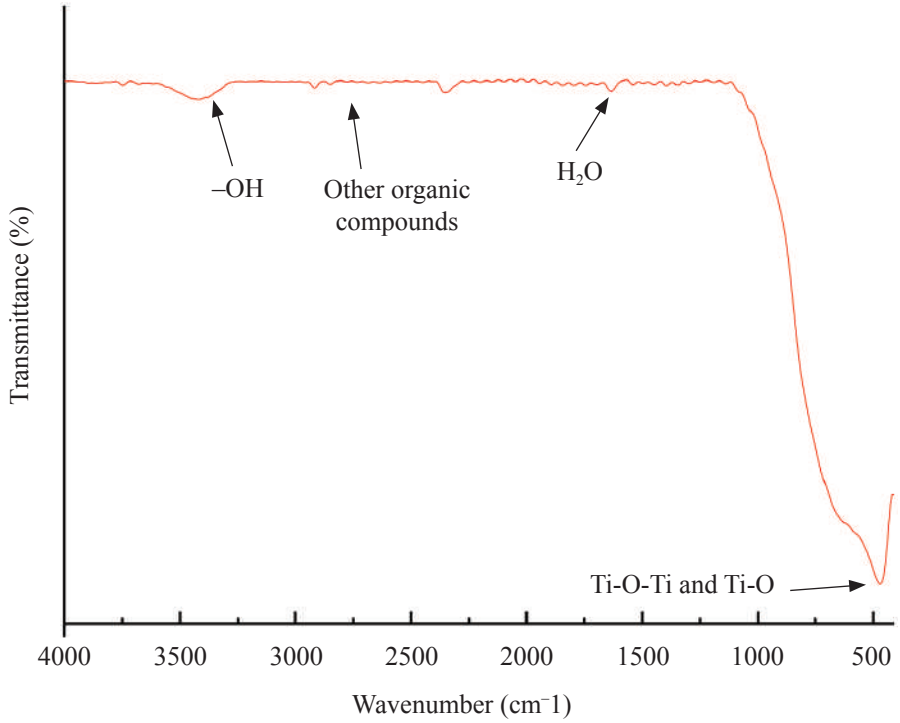

Figure 3. FTIR spectra of synthesized TiO_2 by sol gel method.

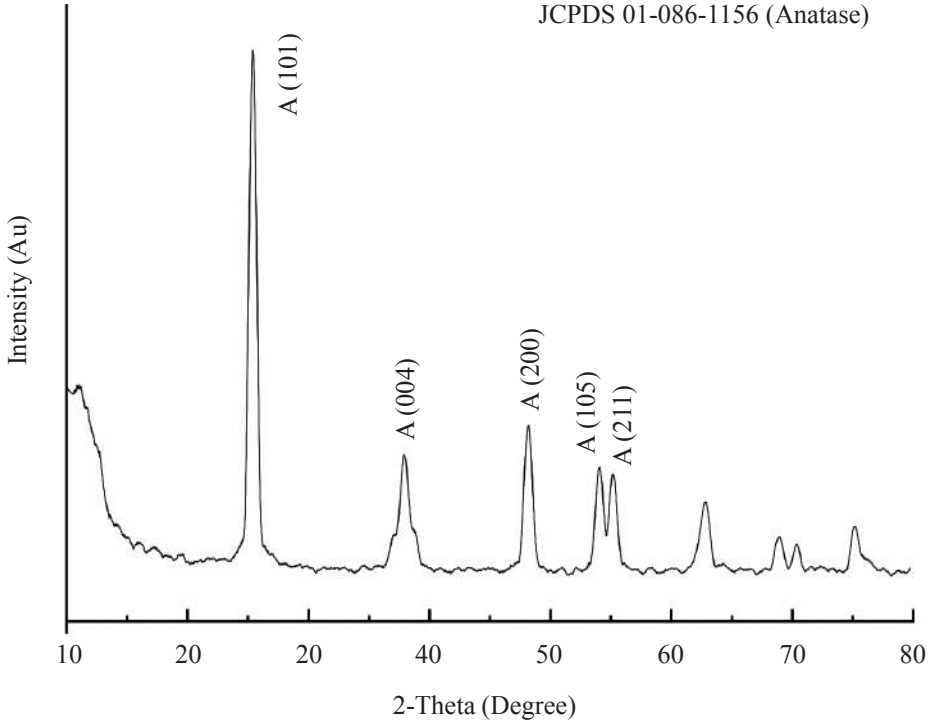

Figure 4. The XRD diffractogram for TiO_2 nanoparticles calcined at temperature of 500°C for 5 h.

Scherrer equation according to the XRD data obtained and related to the previous journal (JCPDS 01-086-1156). Figure 5 was tabulated in Table 2 for comparison of synthesized TiO_2 with the ones from previous literature [12, 16]. It was found that, the average crystallite size of TiO_2 for this study is 26.59 nm.

Table 1. XRD – number of hkl and FWHM to search and calculated number of crystallite size of TiO_2.

Hkl	FWHM	Crystallite size
101	0.0069	22.35nm
004	0.0055	32.23 nm
200	0.0082	25.20 nm
	Average crystallite size	**26.59 nm**

The Raman spectra shows that all synthesized catalysts exhibited anatase phase as reported by literature (Figure 6). The wavenumber appeared in the Raman spectra has been tabulated in Table 3. Comparing the Raman spectra obtained with the reference TiO_2 reported elsewhere [12], it was clear that the Raman bands shift towards higher wavenumber has been observed (Figure 6). The spectra shows a good agreement with TiO_2 in anatase phase. Based on previous research/ literature and their general perception (refers to the studies), said that anatase TiO_2 has a higher photocatalytic activity compared to rutile TiO_2 due to the charge carriers excited deeper in the bulk, thus contributing to the surface reactions in anatase than in rutile [13]. The result obtained

Figure 5 and **Table 2.** XRD patterns of anatase and rutile TiO_2 samples calcined at different temperatures [12].

XRD Shift	Anatase	Rutile
400°C	101, 103, 004, 112, 200, 105, 211, 204, 116, 220, 215	110, 101, 200, 111, 210, 211, 220, 002, 310, 301, 112
500°C	101, 103, 004, 112, 200, 105, 211, 204, 116, 220, 215	110, 101, 200, 111, 210, 211, 220, 002, 310, 301, 112
600°C	101, 103, 004, 112, 200, 105, 211, 204, 116, 220, 215	110, 101, 200, 111, 210, 211, 220, 002, 310, 301, 112
700°C	101, 103, 004, 112, 200, 105, 211, 204, 116, 220, 215	110, 101, 200, 111, 210, 211, 220, 002, 310, 301, 112

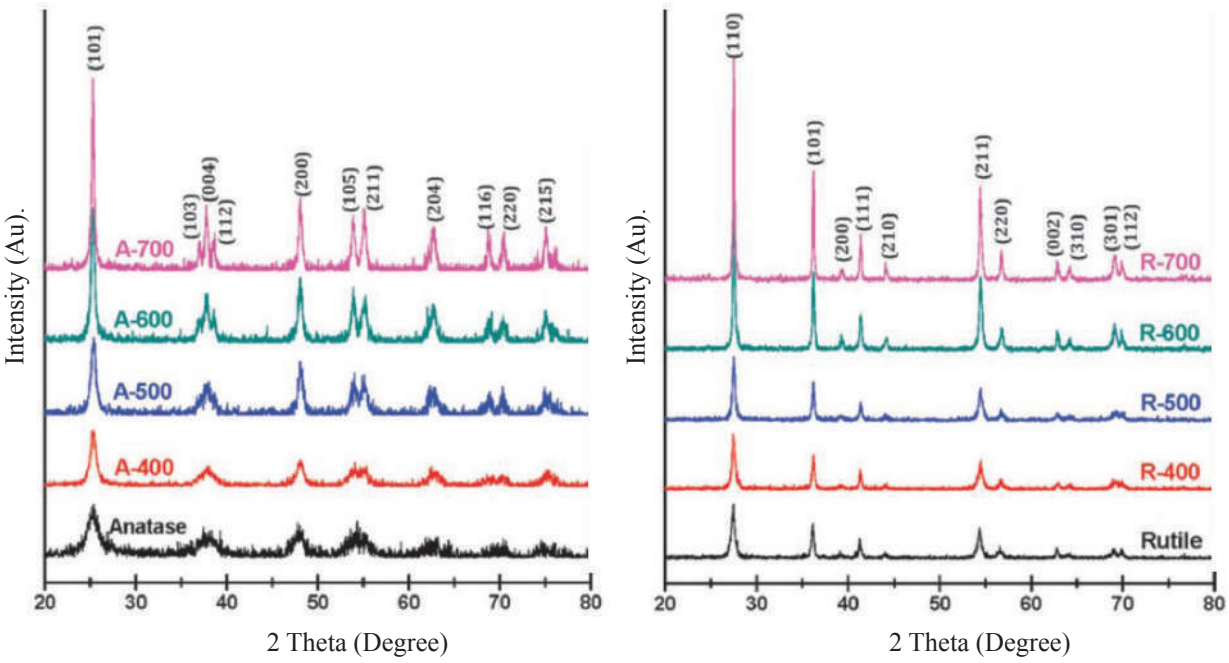

Table 3. Raman spectra of anatase and rutile TiO_2 samples calcined at different temperatures-based on previous literature [12].

Raman shift	Anatase (Wavelength, cm^{-1})	Rutile (Wavelength, cm^{-1})
400ºC	140, 395, 515, 635	230, 445, 610
500ºC	140, 395, 515, 635	230, 445, 610
600ºC	140, 395, 515, 635	230, 445, 610
700ºC	140, 395, 515, 635	230, 445, 610

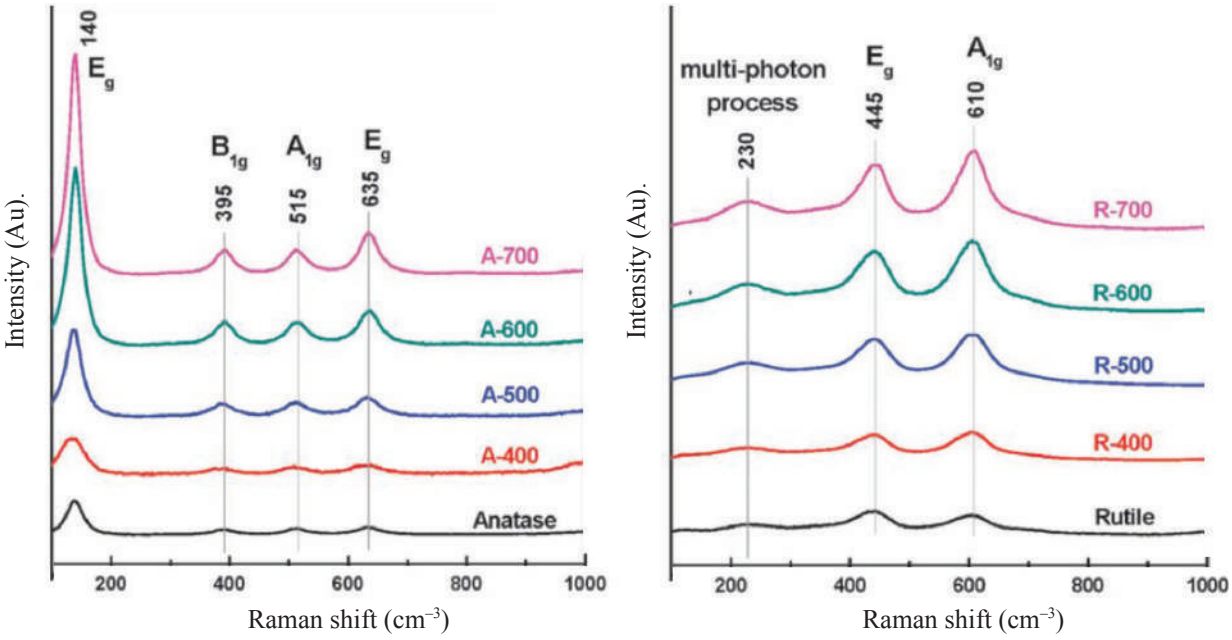

Figure 6. Raman spectra of anatase (left side) and rutile (right side) TiO_2 [12].

from Figure 7 was agreeable to the previous literatures that analyzed anatase conformations of TiO_2. Raman spectra recorded the optimal TiO_2 samples, shown in Figure 7, identified the formation of single anatase nanocrystalline phase. The size of the nanocrystals was estimated to be ~7 nm by projecting the values of the frequency or wavenumber at 145 cm^{-1} of the strongest low frequency of A1 peak (Figure 7) in standard correlation curves [14]. This peak presents blue shift and line broadening relative to that observed in anatase to nanocrystals of large size (more than 20 nm) due to the breakdown of the k = 0 Raman selection rule induced by phonon confinement [14].

Photocatalytic Activity of Adsorption-photodegradation by Cs–TiO_2/Glass

Prior to adsorption-photodegradation process, calibration curve of the MO was performed. The calibration curve was plotted according to the various concentration of the selected MO ranging from 1–20 mg/l. From this calibration plot, the liner equation was determined and could be used to evaluate the photocatalytic degradation efficiency by the prepared photocatalysts. The absorbance of each sample was measured to determine the concentration left after photodegradation process was completed.

The photocatalytic degradation of MO in wastewater utilizing TiO_2 is initiated by light of

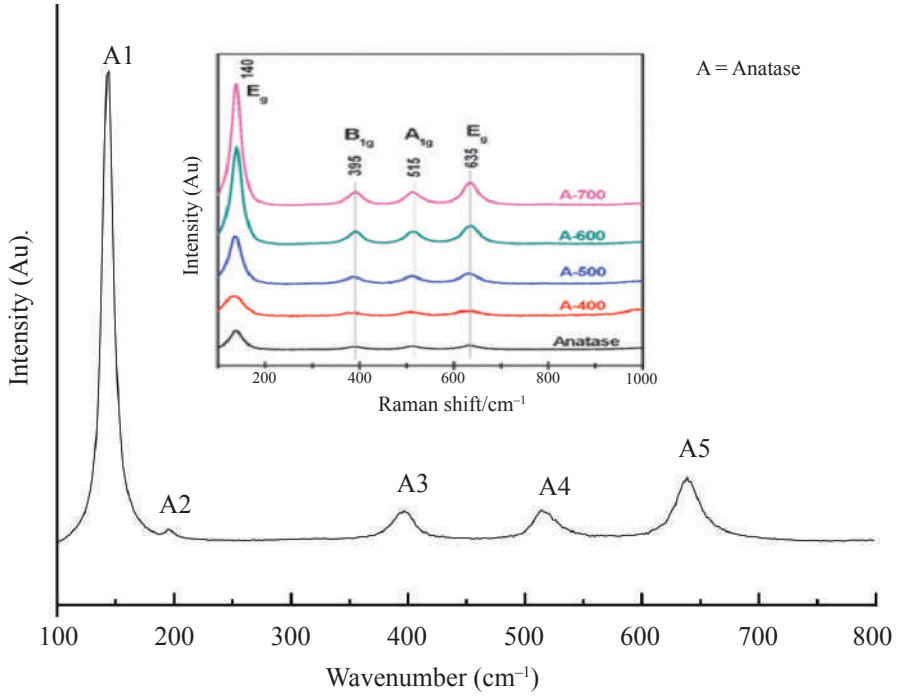

Figure 7. The Raman diffractogram for TiO_2 nanoparticles (synthesis by sol-gel method) was prepared by calcination process at temperature of 500°C for 5 h, comparison with previous literature [12].

wavelength 390nm (3.2eV) [6]. After finishing that process, the next step is to generate positive holes and free electrons, the electrons will be excited from the valence band to the conduction band. The electron–hole pairs will be produced by reactions of oxidation and reduction which can be used to recombine or interact with MO substrates on the surface of TiO_2 particles. To produce the highly reactive oxidizing hydroxyl radicals (•OH) in aqueous solution, the positive holes tend to be cleaned by surface hydroxyl groups which can undergo a degradation process and subsequently lead to the total mineralization of the MO substrate [6].

Mostly, determination of the degradation mechanism of MO as pollutant are used under ultra-violet (UV) or visible light irradiation. This approach was suggested as a new method for the treatment or pre-treatment of dye-containing wastewater. The process is inspired by the principle of photosensitization of wide band gap semiconductors. When a coloured organic compound is present, which is MO in this case, the adsorbed MO molecule is excited by visible light, thus acts as a photosensitizer capable of injecting an electron into the conduction band of semiconductor particles to form an oxidized radical. The oxidized form of the MO molecules will then undergo further degradation. Further mechanism of MO degradation under visible light irradiation is explained by Equations. (2) – (7) [6]:

$$MO + h\nu \rightarrow MO* \quad (2)$$

$$MO* + TiO_2 \rightarrow MO^{\bullet+} + TiO_2(e) \quad (3)$$

$$TiO_2(e) + O_2 \rightarrow TiO_2 + O2^{\bullet-} \quad (4)$$

$$O2^{\bullet-} + TiO_2(e) + 2H^+ \rightarrow H_2O_2 \quad (5)$$

$$H_2O_2 + TiO_2(e) \rightarrow {}^{\bullet}OH + OH^- \quad (6)$$

$$MO^{\bullet+} + O_2(\text{or } O2^{\bullet-} \text{ or } {}^{\bullet}OH) \quad (7)$$

$\rightarrow$ peroxylated or hydroxylated intermediates

$\rightarrow\rightarrow$ degraded or mineralized products

Adsorption-photodegradation reaction to removed MO. The photocatalytic activity of MO (10 ppm) was performed by using Cs-TiO_2/glass photocatalyst that had been initialised

with adsorption process in dark condition for 15 min and after that, it was irradiated under UV-light lamp (λ = 365 nm) for a period of 60 min. Basically, the TiO_2 photocatalysts synthesized with the addition of Cs exhibited high performance of adsorption where it gave about 60% of MO adsorption by optimum condition of Cs-TiO_2/glass. It is evident that adsorption capability of Cs had not reached its maximum limit. The use of Cs seeing that host material can be done due to the consistency of their chemical design for developing of TiO_2 nanoparticles along with limiting their size, along with for controlling the nanoparticles dispersion. Cs provides unique components related towards the acetylated along with nonacetylated residues inside chitosan matrix, triggering the macromolecular design of Cs to obtain both comparatively hydrophobic along with hydrophilic sites, respectively. Also, Cs will be able to transform their chains by stretched stores into coils and additional transform straight into intertwisted coils along with hydrophobic minuscule domains during the aggregation method, and this macromolecule design of intertwisted coils gets compact and also the movement from the macromolecule is restricted [9]. Furthermore, the Cs-iO_2/glass photocatalyst produced about 70% of MO degradation by optimum condition of Cs-TiO_2/glass.

Effect of different layers of TiO_2/Cs photocatalyst on MO photodegrdadation. A number of experiments were executed to examine the particular ideal prompt packing intended for MO removal through different number of dip-coating of Cs-TiO_2/glass which were 2, 4, 6 and 8 layers. Figure 8 shows that the adsorption-photodegradation of Cs-TiO_2/glass with different layers which were 2 layers, 4 layers, 6 layers and 8 layers towards 10 ppm of MO. Approximately, about 60% of the MO was absorbed first (15 min absorption) and follow by the photodegradation (60 min degradation) of the MO which increased up to 10% by the highest layers which were 8 layers (the optimum condition). Overall total removal of the MO by the 8 layers of film were 70% as compared to the 2 layers, 4 layers and 6 layers which were 30%, 60% and 52%, respectively. It was shown that the optimum adsorption as well as photodegradation occurred effectively with 8 layers of Cs-TiO_2/glass towards MO. Thus, the MO removal was influenced by the high and abundant amount or layers of the catalyst coated on the film/glass.

Interestingly, adsorption capability increased with increasing Cs-TiO_2 loading from 2 layers (30%), 4 layers (60%), 6 layers (52%) until the 8 layers (70%). Examination of the data presented suggested that the combination effect of adsorption-photodegradation by 8 layers of Cs-TiO_2/glass was more preferable to the highest value of MO photodegradation obtained, because the chelating groups (the $–NH_2$ and –OH groups) on the Cs were the attributed group that could be applied to the binding ability or adsorption of that Cs towards MO.

Effect different ratios of TiO_2/Cs photocatalyst on MO photodegradation. A number of experiments were executed to examine the particular ideal prompt packing intended for MO removal through different amount/weight of TiO_2 (synthesis by sol-gel method) which were 0.125 g, 0.25 g, 0.375 g and 0.5 g. From Figure 9, adsorption-photodegradation of Cs-TiO_2/glass with different amount/weight of TiO_2 towards 10 ppm of MO. Approximately, about 74% of the MO was absorbed first (15 min absorption) and followed by the degradation (60 min degradation) of the MO which increased up to 10% by the 2E2 film with an amount approximately about 0.25 g of TiO_2 with 0.25 g of Cs. Overall total removal of the MO by the 2E2 film was 84% compared to 2E1, 2E3 and 2E4 which were 63%, 71% and 75% respectively, which showed that lower removal of MO. Thus, the MO removal was influenced by optimum amount/weight of TiO_2 coated in the 2E2 film/glass.

Interestingly, suitable adsorption capability by Cs was optimized at 0.25 g and was used in 2E1 film (63%), 2E2 film (84%), 2E3 film (71%) and 2E4 film (75%). Examination of the data presented in the graph might suggest that the combination effect of adsorption-photodegradation by 2E2 film or glass was more preferable to the highest value of MO photodegradation which was obtained.

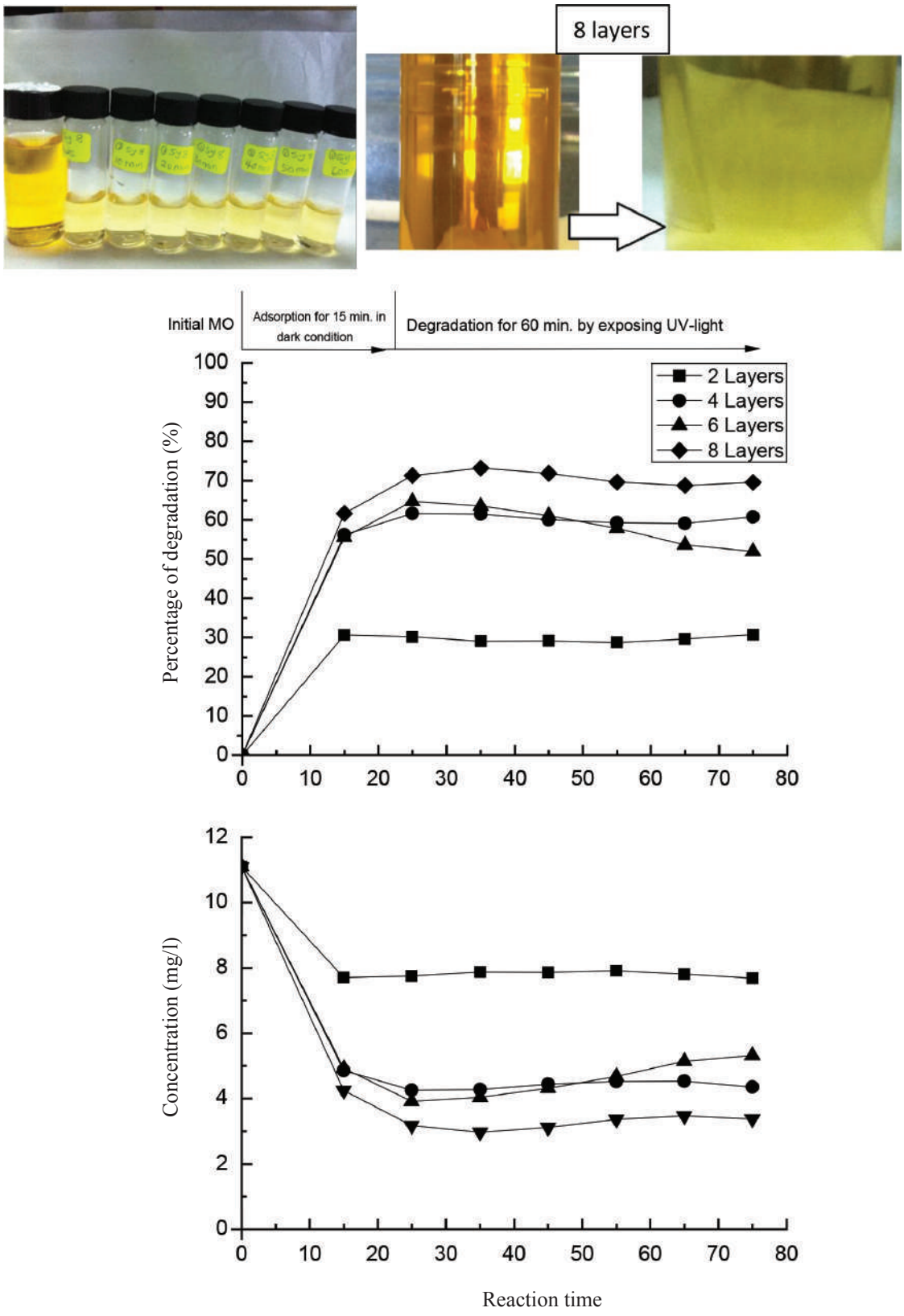

Figure 8. Percentage of photocatalytic adsorption-photodegradation of MO for 75 min by using photocatalyst of Cs-TiO_2/glass and reduced concentration of the MO by those photocatalysts, [MO] = 10 ppm; λ_{UV} = 365 nm.

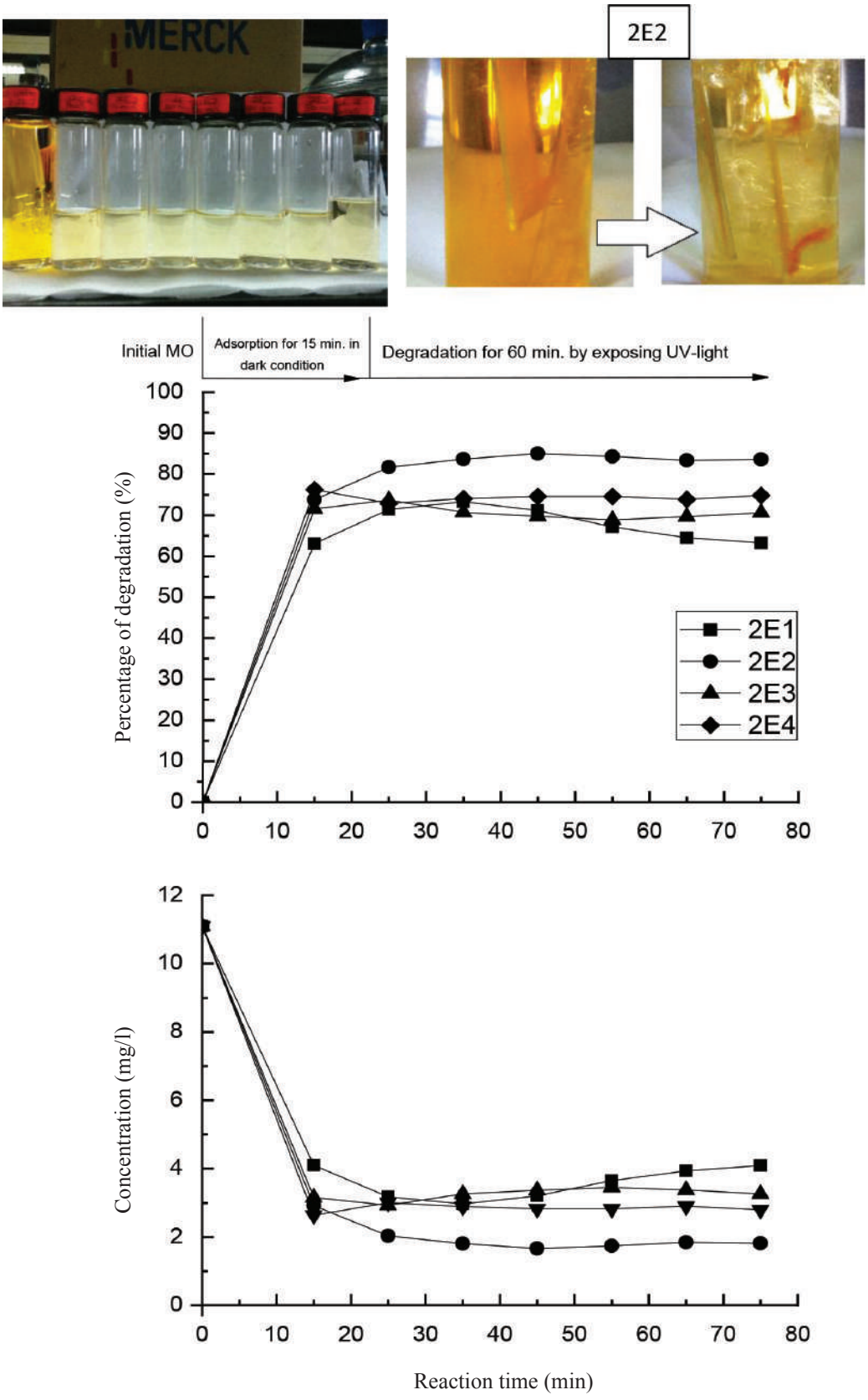

Figure 9. Percentage of photocatalytic adsorption-photodegradation of MO for 75 min by using photocatalyst of Cs-TiO_2/glass and reduced concentration of the MO by those photocatalysts, [MO] = 10 ppm; λ_{UV} = 365 nm.

CONCLUSION

In this study, the photocatalytic activity for degradation of MO solution was conducted using Cs-TiO_2/glass photocatalyst in the presence of UV-light as the energy source. Based on the TGA analysis, the synthesized TiO_2 was determined to be calcined at 500°C. Furthermore, the XRD and Raman analysis revealed that TiO_2 prepared photocatalysts were mostly in crystalline region with anatase phase. Based on the FTIR results, it was observed that the synthesized sample was pure TiO_2.

The photocatalysts Cs-TiO_2/glass was analyzed under optimum conditions with various layers of coating of Cs-TiO_2 and weight ratio of TiO_2 on the glass used, respectively. The obtained results indicated that photocatalysts loading or the number of layers played an important role in determining the removal efficiency of MO attributable to both the adsorption and photodegradation process. A ratio of 0.25 g synthesized TiO_2:0.25 g Cs was identified to give the optimum adsorption-photodegradation of that Cs-TiO_2/glass photocatalyst. Overall, the percentage of adsorption-photodegradation using Cs-TiO_2/glass photocatalyst with the optimum condition of 8 layers and weight ratio of 2E2 (2:2) could contribute to the highest degradation rate reached at 84% of the MO solution.

ACKNOWLEDGEMENT

This work was financially supported by University Malaya Research Grant (UMRG RP022-2012E) and the Fundamental Research Grant Scheme (FRGS: FP049-2013B) by the University of Malaya and Ministry of Higher Education (MOE), Malaysia.

REFERENCES

1. Liu, H., Ramnarayana, R. and Logan, B. E. (2004) Production of electricity during waste water treatment using a single chamber microbial fuel cell, *Environment Science & Technology*, **38**, 2281–2285.
2. Belay K. and Hayelom A. (2014) Removal of methyl orange from aqueous solutions using thermally treated egg shell (locally available and low cost biosorbent), *Innovative Space of Scientific Research Journals*, **1**, 43–49.
3. Gandini, O., Mahe, E., Michaud, P. A., Haenni, W., Perret, A. and Comninellis, C. (2000) Oxidation of carboxylic acids at boron doped diamond, electrodes for waste water treatment, *Journal of Applied Electrochemistry*, **30**, 1345–1350.
4. Pastrana-Martínez, L. M., Morales-Torres, S., Kontos, A. G., Moustakas, N. G., Faria, J. L., Doña-Rodríguez, J. M. and Silva, A. M. (2013) TiO_2, surface modified TiO_2 and graphene oxide-TiO_2 photocatalysts for degradation of water pollutants under near-UV/Vis and visible light, *Chemical Engineering Journal*, **224**, 17–23.
5. Byranvand, M. M., Kharat, A. N., Fatholahi, L. and Beiranvand, Z. M. (2013) A review on synthesis of nano-tio$_2$ via different methods, *Journal of Nanostructures*, **3**, 1–9.
6. Zainal, Z., Hui, L. K., Hussein, M. Z., Abdullah, A. H. and Hamadneh, I (M. K.). R. (2009) Characterization of TiO_2-Chitosan/glass photocatalyst for the removal of a monoazo dye via adsorption–photodegradation process, *Journal of Hazardous Materials*, **164**, 138–145.
7. Bagheri, S., Shameli, K. and Abd Hamid, S. B. (2012) Synthesis and characterization of anatase titanium dioxide nanoparticles using egg white solution via sol-gel method, *Journal of Chemistry*, 2013.
8. Chaudhary, V., Srivastava, A. K. and Kumar, J. (2011) On the sol-gel synthesis and characterization of titanium oxide nanoparticles, *Materials Research Society*, 1352.
9. Fajriati, I., Mudasir, Wahyuni, E. T. (2013) Room-temperature synthesis of TiO_2-chitosan nanocomposites photocatalyst, *The Third Basic Science International Conference*, C10–2.
10. Ahmad, A., Awan, G. H. and Aziz, S. (n.d) Synthesis and applications of TiO_2 nanoparticles. *Department of Metallurgical and Materials Engineering University of Engineering and Technology, Lahore*, **676**, 404–411.
11. Mahata, S. and Kundu, D. (2009) Hydrothermal synthesis of aqueous nano-TiO_2 sols, *Materials Science-Poland*, **27**, 2.
12. Yan, J., Wu, G., Guan, N., Li, L., Li, Z. and Cao, X. (2013). Understanding the effect of surface/bulk defects on the photocatalytic activity of TiO_2: anatase versus rutile, *Phys.Chem. Chem. Phys*., **15**, 10978.
13. Luttrell, T., Halpegamage, S., Tao, J., Kramer, A., Sutter, E. and Batzill, M. (2014) Why is anatase a

better photocatalyst than rutile?-Model studies on epitaxial TiO_2 films, *Scientific Reports*, **4**.

14. Moustakas, N. G., Kontos, A. G., Likodimos, V., Katsaros, F., Boukos, N., Tsoutsou, D. and Falaras, P. (2013) Inorganic–organic core–shell titania nanoparticles for efficient visible light activated photocatalysis, *Applied Catalysis B: Environmental*, **130**, 14–24.
15. Baiju, K. V., Shukla, S., Biju, S., Reddy, M. L. P. and Warrier, K. G. K. (2009) Morphology-dependent dye-removal mechanism as observed for anatase-titania photocatalyst, *Catal. Lett.,* **131**, 663–671.
16. Sanchez, E., Lopez, T., Gomez, R., Bokhimi, Morales, A. and Novaro, O. J. (1996) Synthesis and characterization of sol–gel Pt/TiO_2 catalyst, *Solid State Chem*., 122–309.
17. Gu, Q., Zhu, K., Liu, J., Liu, P., Cao, Y. and Qiu, J. (2014) Rod-like NaNbO3: mechanisms for stable solvothermal synthesis, temperature-mediated phase transitions and morphological evolution, *RSC Advances*, **4(29)**, 15104–15110.